AMPA glutamate receptors are required for sensory-organ formation and morphogenesis in the basal chordate

Shinobu Hirai[a,1], Kohji Hotta[b,1], Yoshihiro Kubo[c], Atsuo Nishino[d], Shigeo Okabe[e], Yasushi Okamura[f], and Haruo Okado[a,2]

[a]Department of Brain Development and Neural Regeneration, Tokyo Metropolitan Institute of Medical Science, Setagaya, Tokyo 156-0057, Japan; [b]Department of Biosciences and Informatics, Faculty of Science and Technology, Keio University, Kohoku, Yokohama, 223-8522, Japan; [c]Division of Biophysics and Neurobiology, Department of Molecular Physiology, National Institute for Physiological Sciences, Okazaki, Aichi 444-8585, Japan; [d]Department of Biology, Faculty of Agriculture and Life Science, Hirosaki University, Hirosaki, Aomori 036-8561, Japan; [e]Department of Cellular Neurobiology, Graduate School of Medicine, The University of Tokyo, Bunkyo-ku, Tokyo 113-0033, Japan; and [f]Department of Biology, Graduate School of Science, Osaka University, Toyonaka, Osaka 560-0043, Japan

Edited by Gail Mandel, Oregon Health and Science University, Portland, OR, and approved January 25, 2017 (received for review August 4, 2016)

AMPA-type glutamate receptors (GluAs) mediate fast excitatory transmission in the vertebrate central nervous system (CNS), and their function has been extensively studied in the mature mammalian brain. However, GluA expression begins very early in developing embryos, suggesting that they may also have unidentified developmental roles. Here, we identify developmental roles for GluAs in the ascidian *Ciona intestinalis*. Mammals express Ca^{2+}-permeable GluAs (Ca-P GluAs) and Ca^{2+}-impermeable GluAs (Ca-I GluAs) by combining subunits derived from four genes. In contrast, ascidians have a single *gluA* gene. Taking advantage of the simple genomic GluA organization in ascidians, we knocked down (KD) GluAs in *Ciona* and observed severe impairments in formation of the ocellus, a photoreceptive organ used during the swimming stage, and in resorption of the tail and body axis rotation during metamorphosis to the adult stage. These defects could be rescued by injection of KD-resistant GluAs. GluA KD phenotypes could also be reproduced by expressing a GluA mutant that dominantly inhibits glutamate-evoked currents. These results suggest that, in addition to their role in synaptic communication in mature animals, GluAs also have critical developmental functions.

AMPA-type glutamate receptor | morphogeneis | ascidian | development

Glutamate has been proposed to regulate neural development via nonsynaptic mechanisms, either by directly activating ionotropic and/or metabotropic glutamate receptors expressed on neural progenitors or indirectly by inducing neighboring cells to secrete molecules regulating neurogenesis, such as neurotropic factors (1–3). The early onset of AMPA-type glutamate receptor (GluA) expression in developing embryos also raises the possibility of other currently unidentified roles. For example, mouse gluA transcripts are detectable by embryonic day 10, and in zebrafish, zygotic gluA transcripts are expressed as early as the midblastula stage (4–10). These observations, combined with in vitro results, suggest a role for GluAs in neural cell proliferation (11, 12). In vertebrates, GluAs form tetramers consisting of various combinations of four subunits (GluA1–GluA4) (13–15). The presence of four *gluA* genes has prevented efficient generation of mice with all four genes deleted. Therefore, the precise role of GluAs in early development of neural and nonneural tissue has not yet been determined in vivo.

Here, we instead used the ascidian chordate *Ciona intestinalis*, the closest living relative to vertebrates (16), which is thought to have just a single *gluA* gene (17). *Ciona* larvae are transparent, enabling easy identification of cells expressing a target gene and detection of morphological phenotypes in the tissues and organs. The *Ciona* life cycle consists of two main phases: a short larval phase with a vertebrate-like notochord, which lasts until about 27 h postfertilization (hpf), and a nonmotile adult phase, which occurs after metamorphosis and lasts about 3–6 mo. After rapid embryogenesis, hatched larvae are able to swim for a few hours (17.5–24 hpf) (18, 19). During this stage, *Ciona* have a photoreceptive organ, the ocellus, which allows them to respond to light. Decreasing light induces swimming, whereas increasing light causes larva to stop swimming and settle onto substrates (20, 21). During the larval period, larvae prepare for the onset of metamorphosis, which usually begins with adhesion (24–27 hpf) (18, 19), followed, in turn, by tail regression into the trunk region (27–29 hpf), body-axis rotation (30–60 hpf), and the formation of adult organs including gill slits, the endostyle, and the digestive tract (22).

In this study, taking advantage of the simple genomic organization of ascidians, we provided convincing evidence that GluAs are essential for normal body development in vivo, including the formation of sensory organs and metamorphosis. We also indicated a critical role for ionotropic glutamate receptors in early development requiring ion flux through GluAs.

Significance

In mammals, AMPA-type glutamate receptors (GluAs) are expressed ubiquitously in the central nervous system and play critical roles in synaptic plasticity, learning, and memory. Here we examined GluAs in the ascidian, *Ciona intestinalis*, and determined that they are expressed in a limited subset of cells during early development. We further find that GluAs are required for development of the ocellus, a photoreceptive organ used during the swimming stage, and for tail resorption and body axis rotation during metamorphosis. These functions require ion influx through GluAs. This is a demonstration of an in vivo requirement for GluAs in organ formation and morphogenesis. GluAs are also expressed during mammalian development, suggesting that developmental roles of GluAs may be functionally conserved.

Author contributions: S.H., K.H., and H.O. designed research; S.H., K.H., Y.K., and A.N. performed research; S.H. and A.N. contributed new reagents/analytic tools; Y.O. and H.O. supervised research; S.H. and K.H. analyzed data; and S.H., Y.K., S.O., and Y.O. wrote the paper.

The authors declare no conflict of interest.

This article is a PNAS Direct Submission.

Data deposition: The sequences reported in this paper have been deposited in DDBJ/EMBL/GenBank [accession nos. LC070681 (*Ciona* glutamate receptor variant 1), LC070682 (*Ciona* glutamate receptor variant 2), and LC152057 (*Ciona* TARP)].

[1]S.H. and K.H. contributed equally to this work.

[2]To whom correspondence should be addressed. Email: okado-hr@igakuken.or.jp.

This article contains supporting information online at www.pnas.org/lookup/suppl/doi:10.1073/pnas.1612943114/-/DCSupplemental.

Results

Analysis of the *Ciona* genome database and molecular cloning confirmed that *Ciona* has just a single GluA subunit with two splice variants at the C terminus (Fig. S1). Notably, clear zygotic expression of *cigluA* and the glutamate aspartate transporter (*glast*) starts at the neurula stage (7 hpf), whereas the expression of the vesicular glutamate transporter (*vGlut*) starts at the mTb (midtailbud) (11 hpf) stage. The neurula stage is when neuronal differentiation occurs. Compared with GluAs from other invertebrate species, the ciGluA sequence has the highest homology to mouse GluAs (Fig. 1*B*). In situ hybridization revealed ciGluA transcripts located in a restricted region behind the ocellus from the early tailbud stage and the hatching larval stage (Fig. 2 *A–A”*, arrow and brackets). To further characterize the identity and morphology of ciGluA-expressing cells, we created a reporter plasmid expressing GFP under the control of the cigluA promoter (cigluAp–GFP) (Fig. 1 *C–C”’*). Electroporation of cigluAp-GFP into *Ciona* fertilized eggs resulted in expression of GFP in specific cell populations. In vertebrates, GluA expression is observed throughout the CNS (23–25). Intriguingly, among the ∼100 neurons present in the CNS of *Ciona* (26), only about 10 were GFP-positive (Fig. 2 *B–D*). GFP signals showed patterns similar to *gluA* mRNA expression patterns in hatched larvae. The morphology of GFP-positive cells behind the ocellus indicated that they are neurons, with axons extending toward the motor ganglion (located between the head/trunk and tail) (Fig. 2 B–D). A few other GFP-positive cells colocalized with arrestin-positive photoreceptor cells in the ocellus (Fig. 2 *C*, *C’*, and *D*). Arrestin is a key protein for termination of the rhodopsin active state (27).

To explore the function of GluAs during development, we knocked down (KD) *ciGluA* expression using a morpholino oligonucleotide (MO), a stable oligonucleotide that inhibits mRNA translation starting from the fertilized egg stage. No morphological differences in ciGluA-expressing cells were observed at 14 hpf (Fig. S3 *A* and *B*). However, 8 h later (22 hpf), axonal extension from ciGluA-expressing cells had been arrested (Fig. S3 *C* and *D*), and arrestin-positive photoreceptor cells were absent from the KD larvae (Fig. 3 *A* and *B*). The larval ascidian ocellus consists of melanin-containing pigment cells and vertebrate-type photoreceptor cells (28, 29). Loss of ciGluAs did not influence the development of pigment cells (Fig. 3 *A* and *B*). We also measured intact GFP intensity before immunostaining in 20 hpf larvae and detected about 2.8-fold weaker intensity in MO-injected larvae than in control larvae (Fig. S3*E*).

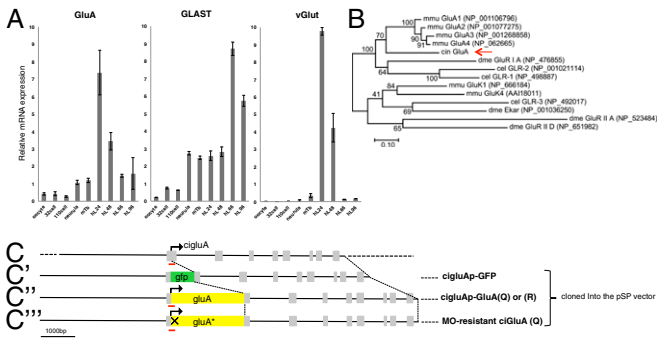

Fig. 1. Characterization of *Ciona* GluA. (*A*) Quantification of CiGluA, ciGLAST, and ci vGlut transcripts at the indicated developmental stage measured by quantitative real-time RT PCR. Equal amounts of total RNA were used for reverse transcription. More than 100 embryos were used for the analysis at each developmental stage. hpf, hours postfertilization; mTb, midtailbud stage. Data are expressed as the average of three wells plus the SE. (*B*) A maximum-likelihood tree of the various GluA proteins (cel, *C. elegans*; cin, *C. intestinalis*; dme, *D. melanogaster*; mmu, *Mus musculus*). The red arrow marks the position of ciGluA protein. Scale indicates 0.10 substitutions per position. (*C*) Schematic diagram of the *cigluA* gene. (*C’–C”’*) Constructs used in this study. (*C’*) Schematic of the cigluA-promoter-GFP (cigluA-GFP) reporter construct. (*C”*) Schematic of the ciGluA expression construct (cigluAp-GluA). (*C”’*) Schematic of the MO-resistant ciGluA expression construct (cigluA-GluA*). Red bars indicate the MO target site that is disrupted in cigluA-GFP reporter construct (*C’*). The cross represents three silent mutations incorporated in the MO-resistant construct.

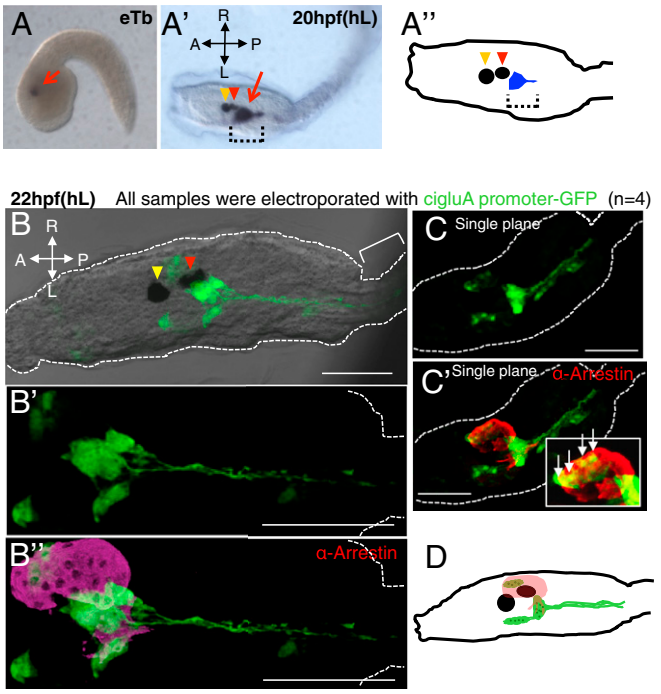

Fig. 2. CiGluA is expressed in only a subset of neurons in the CNS. (*A* and *A’*) ciGluA expression analyzed using in situ hybridization. eTb, early tailbud stage, about 8.45 hpf ($n = 26$); hL, hatched larva at about 20 hpf ($n = 31$). The red arrow in *A* and the dotted brackets in *A’* and *A”* indicate *cigluA* mRNA expression, the yellow arrowheads in *A’* and *A”* indicate the otolith, and the red arrowheads in *A’* and *A”* indicate the ocellus. (*A’*) A schematic diagram illustrating the spatial relationship between *cigluA* mRNA-expressing cells and the otolith and ocellus in hL. (*B–C’*) Hatched larvae were electroporated with cigluA-GFP. (*B*) 3D reconstruction images showing merged DIC and GFP staining. The yellow arrowhead indicates the otolith, and the red arrowhead indicates the ocellus. The bracket indicates part of the tail. (*B’*) Higher magnification image of the GFP staining pattern in *B*. (*B”*) Images costained for GFP and arrestin (a mature photoreceptor marker). (*C*) An independent sample expressing GFP and (*C’*) costained for arrestin. The white box in *C’* is a higher magnification image of the photoreceptor region with arrows indicating cells that coexpress GFP and arrestin. (*D*) Schematic illustrating the spatial relationship between arrestin-positive photoreceptor cells (pink) and ciGluA-promoter–induced GFP-positive cells (green) in hL. The black circle and ellipse represent the otolith and the ocellus, and the dark green dots within the light green areas indicate cell nuclei. (Scale bars, 50 μm.)

At 66 hpf, the process of metamorphosis was severely impaired, resulting in tails that failed to shrink and defective body-axis rotation (Fig. 3 *D* and *E*). These developmental defects were completely rescued by injecting a MO-resistant ciGluA construct, suggesting a specific, rather than off-target, action of the MO (Fig. 3 *C* and *F*). To confirm that disappearance of the photoreceptor marker, arrestin, was accompanied by functional defects, we evaluated shadow-response behavior, which is active swimming caused by an acute loss of light (20, 21). ciGluA KD larvae showed reduced swimming behavior in response to a dark stimulus (Fig. 3*G*). We have demonstrated that GluAs are crucial for normal differentiation of GluA-expressing cells in vivo. Moreover, this is evidence for the indispensability of GluAs in

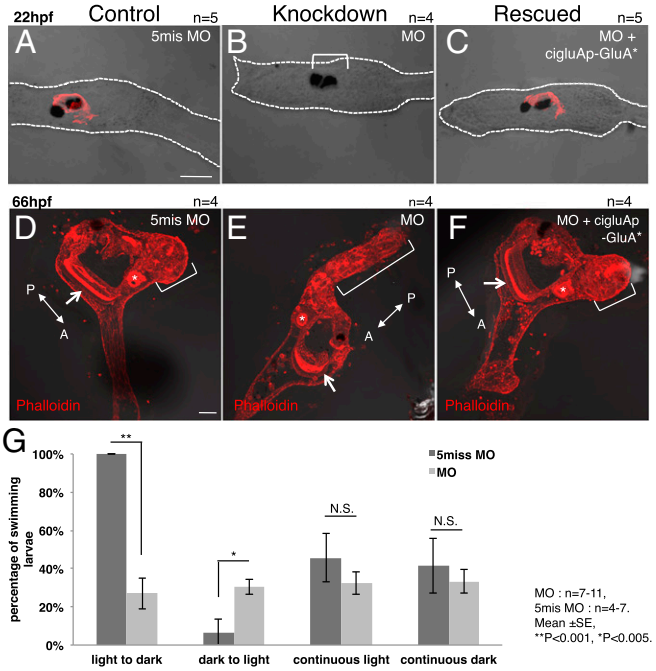

Fig. 3. GluA knockdown leads to defects in sensory-organ differentiation and metamorphosis. (*A* and *D*) Samples injected with control 5mis MO. (*B* and *E*) MO against ciGluA. (*C* and *F*) MO against ciGluA rescued with the MO-resistant ciGluA construct. (*A*–*C*) Hatched larval DIC images merged with arrestin immunostaining. The arrestin signal was almost completely absent in MO-injected larvae (bracket in *B*). (*D*–*F*) Juvenile images showing merged DIC and phalloidin staining (F-actin). The arrow and asterisk in *D*–*F* indicate the endostyle and digestive tract, respectively, showing that internal organs developed normally. The bracket in *E* indicates the tail that failed to shrink. The brackets in *D* and *F* indicate normal, shrunken tails. [Scale bars, 50 μm (*A* and *D*).] (*G*) Percentage of larvae that swam in indicated light conditions. Mean ± SE, $**P < 0.001$, $*P < 0.005$.

organ developmental and behavioral phenotypes, including the formation of sensory organs, sensory-guided swimming behavior, and metamorphosis.

We used the *Xenopus* oocyte expression system to confirm the physiological properties of ciGluAs. CiGluAs did not induce clear inward currents triggered by glutamate (Fig. 4*E*, upper traces). This is not unexpected, as *Caenorhabditis elegans* and *Drosophila melanogaster* GluAs require coinjection of transmembrane GluA regulatory proteins (TARPs) to achieve a glutamate response (30–32). TARPs facilitate the membrane targeting and channel function of GluAs (33, 34). Therefore, we isolated the cDNA for *Ciona* TARP (ciTARP) (Fig. S4) and coexpressed it with ciGluA in *Xenopus* oocytes (Fig. 4*E*, lower traces). The amplitude of glutamate-evoked responses was relatively small, but this may be explained either by the requirement of additional auxiliary proteins or by the intrinsic ion permeability of the ciGluAs (Fig. 4 *F* and *G*, left column).

Mammalian GluAs can be divided into two classes based on of Ca^{2+} permeability. Ca^{2+} permeability depends on the substitution of a single amino acid residue in the ion channel pore from glutamine (Q) to arginine (R) by RNA editing (called Q/R editing) (1–3, 35–38). GluAs that include the R-type GluA2 subunit lack Ca^{2+} permeability (13, 39). In very early development, most mammalian GluAs are Ca^{2+}-permeable GluAs (Ca-P GluAs), but the Ca^{2+}-impermeable GluAs (Ca-I GluAs) population increases rapidly by birth, due to intensive Q/R RNA editing of the GluA2 subunit (40–44). Defects in this process cause serious problems (45–49). Decreased efficiency in Q/R editing is observed in, for example, patients with amyotrophic lateral sclerosis (ALS), leading to increasing Ca^{2+} influx and cell death in motor neurons (45, 46). Mice with genetic manipulations that inhibit Q/R conversion of GluA2 subunits die within a few weeks of birth from epilepsy and excess Ca^{2+} influx into neurons (49). Thus, the presence of R-type receptors is crucial for mammals to survive. To test whether similar Q/R editing and cooperation of Ca-P GluAs and Ca-I GluAs occur in ascidians, we first assessed the Q/R editing status in *Ciona*. No Q/R editing was detected at any of the three developmental stages we selected, suggesting that *Ciona* is likely to have only Q homomultimers (ci-Q/Q) (Fig. S5*A*). We next investigated the electrophysiological properties of ci-Q/Q using *Xenopus* oocytes, which have endogenous Ca^{2+}-activated Cl^- channels. Thus, Ca^{2+} permeability of GluAs can be monitored as a transient outward current through the Cl^- channels (see *Materials and Methods* for details). We demonstrated that ciGluAs are Ca^{2+}-permeable with inward rectification (Fig. S5*B*). The ciGluA Ca^{2+}-permeability index was almost the same as that for rat GluA (Fig. S5*C*). Thus, *Ciona* has only Ca-P GluAs throughout its life span because ciGluAs are the sole AMPA-type receptor in this species. Other invertebrates, such as nematodes and flies, have also been reported to have only Q-type GluAs (50). The requirement for Ca-I GluAs in mammals appears to be evolutionarily unique and may be related to the role of GluAs in synaptic transmission acquired during the evolution of vertebrates.

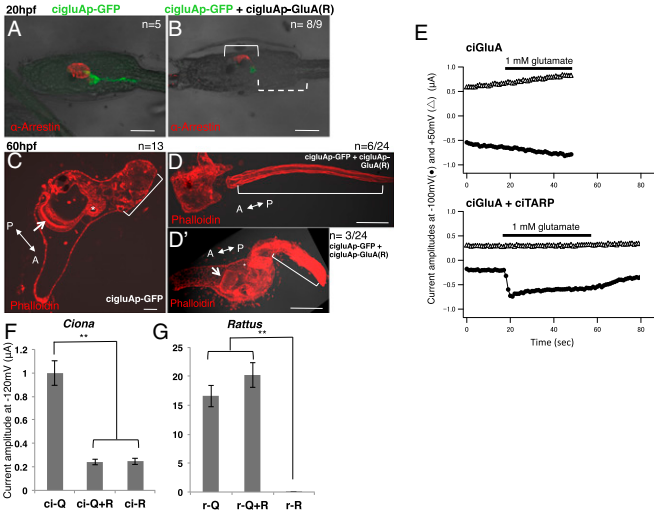

Fig. 4. Artificial *Ciona* R-type GluAs dominantly inhibit activity of Q-type GluAs. (*A* and *B*) DIC images of hatched larvae merged with GFP and arrestin staining patterns. In *B*, the dotted bracket indicates GFP-positive cells with defective axons and the solid bracket indicates partial loss of arrestin-positive photoreceptor cells in an R-type ciGluA electroporated larva. (*C*–*D'*) DIC images merged with F-actin labeling with phalloidin in juveniles. The arrow and asterisk in *C* and *D'* indicate the endostyle and digestive tract, respectively, showing that the internal organs developed normally. The bracket in *D* indicates a cut tail. The bracket in *D'* indicates a tail that failed to shrink. The bracket in *C* indicates a normal, shrunken tail. In control samples, all samples ($n = 13$) showed normal regression. In the R-type ciGluA electroplated samples ($n = 22$), 32% of samples were normal ($n = 7$), and 68% ($n = 15$) showed abnormal tail regression. Among these, seven showed impaired regression, and eight showed no regression. Seven of the eight larvae with no regression had cut tails. [Scale bars, 50 μm (*A*–*C*) and 100 μm (*D* and *D'*).] (*E*) Current flow induced by glutamate application in *Xenopus* oocytes voltage clamped at –100 mV (filled circles) and +50 mV (open triangles). *Upper* plots currents in oocytes injected with cRNA for ciGluA alone, and *Lower* plots currents in oocytes injected with both cRNA for ciGluA and ciTARP. Black bars indicate the timing of glutamate application. (*F* and *G*) The average peak current amplitude after glutamate application in *Xenopus* oocytes injected with only Q-type or R-type, or mixed subunit types (Q/R-hetero). All data were obtained in the absence of extracellular Ca^{2+}, and TARP was coexpressed in all groups. r, rat. $n = 6$–11. Mean ± SE. $**P < 0.001$.

In vertebrates, a single amino acid substitution alters the calcium permeability of GluAs. Does an identical substitution artificially created in ciGluAs similarly alter the properties of the ion channel? To test this, we created a ciGluA construct that was artificially edited at the Q/R site and studied its electrophysiological properties. In the course of characterization of heteromeric AMPA receptors, we uncovered distinct properties of *Ciona* receptors compared with mammalian receptors. Unexpectedly, the current amplitude of Q- and R-hetero multimers (ci-Q/R) was significantly smaller than that of ci-Q/Q multimers and at a similar level to that of ci-R/R multimers (Fig. 4*F*). This is in clear contrast with mammals, where r-R/R is almost nonfunctional and the r-Q/R current is similar to that of r-Q/Q (Fig. 4*G*), as shown previously by Hollmann et al. (13). These results indicate that requirement of Ca^{2+} permeability of ciGluAs during development cannot be examined, whereas the artificial R-type ciGluA subunit functions as a dominant-negative subunit. This enabled us to discriminate between the possible functional and structural roles of GluAs during early development. Specifically, we electroporated an R-type (ci-R) expression construct into fertilized *Ciona* oocytes, which endogenously express only Q-type ciGluAs, expecting the dominant-negative effect of ci-R to result in suppression of GluA-mediated cation influx. Expression of ci-R under the cigluA promoter led to a phenotype similar to, but slightly milder than, that produced by ciGluA KD by MO. At 20 hpf, seven larvae out of the nine showed loss of axonal extension (Fig. S6). Five out of nine larvae electroporated with R-type GluAs had a partial loss of arrestin-positive cells, with three out of those nine larvae showing a loss of arrestin-positive cells resembling the loss in MO experiments (Fig. 4 *A* and *B* and Fig. S6). At 60 hpf, we found two types of defects in metamorphosis. One was similar to defects observed in MO-injected larvae, with defective tail regression but normally developed adult organs (Fig. 4*D'*), and the other consisted of larvae with cut tails and defective adult organs (Fig. 4*D*). In addition, body-axis rotation did not occur in ci-R electroporated larvae (Fig. 4 *D* and *D'*). The observed developmental defects from ci-R induction are caused by reduced ion influx through GluAs (Fig. 4*F*) and not by loss of GluA function as a signal transducer and/or adhesion molecule, which is independent of ion permeability. The fact that vertebrate-like single amino acid substitution of ciGluAs induced dramatic developmental phenotypes in ascidian larvae illustrates the indispensable role of ciGluAs as a glutamate-sensitive ion channel during early development.

Discussion

In this study, we uncovered a unique expression pattern of ciGluAs. In contrast to mammals where GluAs are expressed throughout the CNS (51), expression in *Ciona* is restricted to a small population of neural cells (Fig. 2 *A–D*). This suggests a possibility that GluAs may have originally functioned in development and later transitioned to become a predominant mechanism for synaptic neurotransmission. Consistent with this possibility, we demonstrate that ciGluAs are required for organ formation and dynamic body transformation. Vertebrates have two types of visual systems: lateral paired eyes and parietal or pineal eyes. The *Ciona* ocellus has been reported to be homologous with the pineal eye. First, the ocellus originates from the same part of the neural plate as the vertebrate pineal eye. Both are derived from the lateral part of the neural plate and have a final location in a dorsal part of the anterior brain (52, 53). Second, the ascidian ocellus serves as a photoreceptive organ, necessary for the shadow response (54, 55). Pineal eyes in larval amphibians have the same function (56). In our studies, lack of ciGluAs caused loss of arrestin immunoreactivity and a reduction in shadow-response behavior (Fig. 3 *A*, *B*, and *G*), which suggests that ciGluAs are required for pineal eye-like organ formation and function. Supporting this idea, GluA expression in the pineal body has been reported in macaques and in the developing rat (57, 58). Further experiments, for example, with specific marker antibodies, are needed to confirm whether the ascidian ocellus is indeed homologous with the pineal eye.

CiGluAs are expressed in a subpopulation of photoreceptor cells, and loss of GluA expression or activity results in reduced amounts of arrestin (Figs. 2 *A–D* and 3 *A* and *B*). How does GluA in a subpopulation affect all arrestin-positive cells? The loss of GluAs in photoreceptor cell progenitors in the early stages of development may prevent proliferation of these cells, leading to the absence or reduction of arrestin-positive cells. We observed zygotic expression of ciGluA transcripts at the neurula stage (Fig. 1*A*), whereas arrestin expression starts later, during the early tailbud stage (59). Weak GFP signals in GluA KD cells probably reflect the immaturity of those cells (Fig. S4 *A–E*). In rodents, functional GluAs are expressed in proliferative neural precursor cells in addition to mature neurons (60, 61). However, prior in vitro studies have not identified which cells expressing GluAs are required for progenitor differentiation (11, 12). In the present study, we demonstrated that GluAs are crucial for the development of GluA-expressing cells, as shown by the partial arrestin expression and arrested axonal extension of GluA-expressing cells in promoter-induced ci-R electroporated larvae (Fig. 4 *A* and *B* and Fig. S6). In the course of metamorphosis, only tail regression and body-axis rotation were inhibited by decreased functionality of ciGluAs in our experiments (Figs. 3 *D* and *E* and 4 *C–D'*). This suggests that the other metamorphosis steps are controlled by independent mechanisms and that only tail regression and body-axis rotation are on the same cascade. Several previous studies with mammalian cells in vitro have demonstrated that GluAs contribute to axonal development and cell morphology (62–65). It is possible that the axons that vanished with GluA KD or ci-R electroporation may transmit the signal to start tail regression and body-axis rotation.

Quantitative real-time PCR results (Fig. 1*A*) indicated that *gluA* is expressed at the neurula stage, whereas expression of vGlut, which is required for synaptic transmission, begins later at the mTb stage (11 hpf). Furthermore, GLASTs, which remove extracellular glutamate independently from synaptic function (66–68), are also expressed at the neurula stage. These data suggest that the functions of ciGluA during early development may be independent from GluA's roles in synaptic transmission. Our identification of ascidian GluA suggests that a prototypical *gluA* gene encoded a calcium-permeable channel and may have been associated with calcium signaling involved during development (69, 70). This gene likely later evolved into the four different *gluA* genes (GluA1, GluA2, GluA3, and GluA4) present in mammals that function to depolarize cells through mainly sodium influx.

Materials and Methods

cigluAp-GFP and cigluAp-ciGluA Coding Sequence Construction and Mutagenesis. Following dephosphorylation, a pSP eGFP vector (from Takeo Horie) was cut out by digestion with Pvu II. The ~8 kbp amplified PCR fragment, including the cigluA regulatory sequence (RS) and the ATG start codon, was phosphorylated and cloned into the pSP vector above (termed "pSP cigluA RS vector"). The 8 kbp RS was amplified by PCR with the primers CGATCTTCGGTATCGTAAGAGATCA (Fwd), TTGAAATTTTACCTGGTGTGC (Rev), TTTTACTTCTTTTGTACTCCCGTA (Nested Fwd), and GCGGTGTGCAAAATCGTACT (Nested Rev).

To insert the GFP and cigluA coding sequences (CDSs) under the cigluA RS, restriction site-generating mutagenesis was performed at the start codon site of the RS vector, leading to inhibition of the transcription of exons contained within the 8 kbp RS sequence. The mutagenesis primers were gatcgtcgacCCGGTATGTCCACAGCATTC (Fwd) and gtcAggAtccCACTTGTTGTTACTGCATAA (Rev) (lowercase letters in the primer sequences indicate mismatched nucleotides introduced to generate the restriction site for XbaI).

After digestion with XbaI, blunting, and dephosphorylation, eGFP and cigluA CDS fragments were fused into the pSP cigluA RS sequence. For eGFP, we inserted the Pvu-II–digested eGFP fragments described above.

To make the MO-resistant construct, we used the following primers to generate silent mutations in the cigluA-RS–induced ciGluA CDS construct:

GAATGTCTCGtaGgACTATAAAAATAG (Fwd) and CGAAATTGCATTTGAAACTAT (Rev). Construction images are presented in Figs. 1*C* and 2*C*‴.

Behavioral Test for Light Sensitivity. We evaluated light-sensing behavior in fully matured swimming larvae (22 hpf, st.28 according to FABA2: chordate.bpni.bio.keio.ac.jp/faba2). To produce the dark and light stimuli, we alternately covered and uncovered the larvae with a black plastic sheet. Swimming behavior (movement of the tail from side to side) toward the dark stimulus was recorded with a digital camera (Olympus CAMEDIA SP-350) and scored manually.

Electrophysiology in *Xenopus* Oocytes. After linearization with NheI (ciGluA and ciTARP in the pGEMHE vector) or XhoI [ratGluA2 in the pBlueScript II SK (–) vector], cRNAs were transcribed with a T8 RNA transcription kit (Invitrogen). Rat GluA2Q and 2R vectors were gifts from J. Boulter, University of California, Los Angeles. *Xenopus laevis* were anesthetized in water containing 0.15% tricaine, and oocytes were collected through a surgical procedure, as described previously (71). The isolated oocytes were treated with collagenase (type 1, 2 mg/mL; Sigma) for 6 h and injected with 50 nl of cRNA solution. The amounts of injected cRNA were as follows: ciGluA (25 ng) and ciTARP (0 ng or 25 ng) (Fig. 4*E*), Q [17 ng (Q-only, Q+R) or 0 ng (R-only)], R [0 ng (Q-only) or 17 ng (Q+R, R-only)], and ciTARP [17 ng (all)] (Fig. 4 *F* and *G* and Fig. S5 *B* and *C*). After incubation at 17 °C for 3–4 d in frog Ringer's solution [88 mM NaCl, 1 mM KCl, 2.4 mM NaHCO3, 0.3 mM Ca(NO3)2, 0.41 mM CaCl2, and 0.82 mM $MgSO_4$, pH 7.6, with 0.1% penicillin–streptomycin solution], oocytes were placed in a chamber of a volume of ∼160 μL. Macroscopic glutamate-induced currents were recorded under two-electrode voltage clamp using an OC-725C (Warner Instruments), Digidata 1322A, and pClamp 9.2 (Molecular Devices). Intracellular microelectrodes were filled with 3 M K-acetate and 10 mM KCl and had resistances between 0.2 MΩ and 0.5 MΩ in the standard bath solution, ND96 (98 mM NaCl, 2 mM KCl, 3 mM MgCl2, and 5 mM Hepes, pH 7.4). In the experiments with bath Ca^{2+} (Fig. S4 *B* and *C*), 5 mM CaCl was simply added to the ND96. Oocytes were clamped at −120 mV, and 40 μL of a 5× concentrated stock of glutamate solution was added directly to the bath (160 μL) by pipette. Washout of glutamate was achieved by bath perfusion.

Xenopus oocytes have endogenous Ca^{2+}-activated Cl^- channels (72–74). Thus, Ca^{2+} permeability of GluA can be monitored in oocytes with a high sensitivity. Upon addition of 5 mM Ca^{2+} to the bath, glutamate-evoked Ca^{2+} influx through Q-type ciGluAs activates the Cl^- channels, especially at +60 mV, where Ca^{2+}-induced Cl^- current can be detected better (Fig. S5*B*). The data were analyzed offline in pClamp 9.2, Igor Pro (Wavematrix) and Excel (Microsoft).

All animal experiments involving *X. laevis* in this study conformed to the guidelines of the Animal Care and Use Committee of the National Institute for Physiological Sciences (Okazaki, Japan) and were performed with the approval of the committee.

MO Injection. To inhibit ciGluAs expression, we used the MO technique (Gene Tools). The MO antisense sequence was TAGTACGGCGAGACATTTTAACTGG, and the control MO sequence with five nucleotide mismatches was TAcTAgGGCGAcAgATTTTAACTcG. On the basis of previous studies, 10 fmoles MO in distilled water was injected into intact fertilized eggs (75).

Estimation of Tail Regression. We estimate the regression of tail by the criteria using the ratio of tail length and trunk length; normal regression, 0–0.5; impairment regression, 0.5–2 (shown as a representative in Fig. 4*D*′); no regression, 2< (shown as a representative in Fig. 4*D*). Based on the criteria, in control samples, 100% of samples ($n = 13$) are normal regression. The ratio of 12 samples is 0 and only one sample is 0.1.

Sequence Alignment and Molecular Phylogeny. We used CLC Main Workbench software for amino acid alignment. For molecular phylogenetic analysis, we used MEGA7. Amino acid sequences of the glutamate receptors were aligned by MUSCLE, and a maximum-likelihood tree with 100 replicates of bootstrap analysis was constructed from a dataset of gap-free 350 amino acid alignment covering the S1-TMD4 region.

Animals and handling, quantitative real-time PCR, cloning, Q/R editing status, immunohistochemistry, whole-mount in situ hybridization, accession numbers, and statistics were as described in *SI Materials and Methods*.

ACKNOWLEDGMENTS. We give special thanks to Dr. Takeo Horie (University of Tsukuba, Shimoda, Japan), who gave us the pSP eGFP plasmid and critical advice. The anti-arrestin antibody was a kind gift from Dr. Masashi Nakagawa (University of Hyogo, Kamigori, Japan) and Dr. Horie (University of Tsukuba, Shimoda, Japan). We thank Dr. Hiroki Takahashi (National Institute for Basic Biology, Okazaki, Japan) for providing the ascidian samples for the real-time PCR and in situ hybridization. We also thank Dr. Yoshimichi Murata (Tohoku University) for the pGEMHE plasmid. Rat GluA2 cDNA plasmid was kindly gifted by Dr. James Boulter (University of California, Los Angeles). Dr. Kotaro Oka (Keio University) and Dr. Junjiro Horiuch (Tokyo Metropolitan Institute of Medical Science, Tokyo) kindly gave us helpful discussion. This work was supported by Japan Society for the Promotion of Science KAKENHI Grants 26830033 (to S.H.), 16K07426 and 16H01451 (to K.H.), 25117006 and 26250014 (to S.O.), and 16K14569 and 26290016 (to H.O.) and also by Japan Science and Technology Agency CREST Grant 14529570 (to S.O.).

1. Haydar TF, Wang F, Schwartz ML, Rakic P (2000) Differential modulation of proliferation in the neocortical ventricular and subventricular zones. *J Neurosci* 20(15):5764–5774.
2. Schlett K (2006) Glutamate as a modulator of embryonic and adult neurogenesis. *Curr Top Med Chem* 6(10):949–960.
3. Brazel CY, Nuñez JL, Yang Z, Levison SW (2005) Glutamate enhances survival and proliferation of neural progenitors derived from the subventricular zone. *Neuroscience* 131(1):55–65.
4. Sugden SG, Zirpel L, Dietrich CJ, Parks TN (2002) Development of the specialized AMPA receptors of auditory neurons. *J Neurobiol* 52(3):189–202.
5. Luján R, Shigemoto R, López-Bendito G (2005) Glutamate and GABA receptor signalling in the developing brain. *Neuroscience* 130(3):567–580.
6. Lin WH, Wu CH, Chen YC, Chow WY (2006) Embryonic expression of zebrafish AMPA receptor genes: Zygotic gria2α expression initiates at the midblastula transition. *Brain Res* 1110(1):46–54.
7. Brockie PJ, Madsen DM, Zheng Y, Mellem J, Maricq AV (2001) Differential expression of glutamate receptor subunits in the nervous system of *Caenorhabditis elegans* and their regulation by the homeodomain protein UNC-42. *J Neurosci* 21(5):1510–1522.
8. Métin C, Denizot JP, Ropert N (2000) Intermediate zone cells express calcium-permeable AMPA receptors and establish close contact with growing axons. *J Neurosci* 20(2):696–708.
9. Hoppmann V, Wu JJ, Søviknes AM, Helvik JV, Becker TS (2008) Expression of the eight AMPA receptor subunit genes in the developing central nervous system and sensory organs of zebrafish. *Dev Dyn* 237(3):788–799.
10. Bettler B, et al. (1990) Cloning of a novel glutamate receptor subunit, GluR5: Expression in the nervous system during development. *Neuron* 5(5):583–595.
11. Luk KC, Sadikot AF (2004) Glutamate and regulation of proliferation in the developing mammalian telencephalon. *Dev Neurosci* 26(2-4):218–228.
12. Martins RA, Linden R, Dyer MA (2006) Glutamate regulates retinal progenitors cells proliferation during development. *Eur J Neurosci* 24(4):969–980.
13. Hollmann M, Hartley M, Heinemann S (1991) Ca2+ permeability of KA-AMPA–gated glutamate receptor channels depends on subunit composition. *Science* 252(5007):851–853.
14. Rosenmund C, Stern-Bach Y, Stevens CF (1998) The tetrameric structure of a glutamate receptor channel. *Science* 280(5369):1596–1599.
15. Sobolevsky AI, Rosconi MP, Gouaux E (2009) X-ray structure, symmetry and mechanism of an AMPA-subtype glutamate receptor. *Nature* 462(7274):745–756.
16. Delsuc F, Brinkmann H, Chourrout D, Philippe H (2006) Tunicates and not cephalochordates are the closest living relatives of vertebrates. *Nature* 439(7079):965–968.
17. Okamura Y, et al. (2005) Comprehensive analysis of the ascidian genome reveals novel insights into the molecular evolution of ion channel genes. *Physiol Genomics* 22(3):269–282.
18. Cloney RA (1982) Ascidian larvae and the events of metamorphosis. *Am Zool* 22:817–826.
19. Degnan BM, Souter D, Degnan SM, Long SC (1997) Induction of metamorphosis with potassium ions requires development of competence and an anterior signalling centre in the ascidian Herdmania momus. *Dev Genes Evol* 206(6):370–376.
20. Svane IB, Young CM (1989) The ecology and behavior of ascidian larvae. *Oceanogr Mar Biol Annu Rev* 27:45–90.
21. Tsuda M, Kawakami I, Shiraishi S (2003) Sensitization and habituation of the swimming behavior in ascidian larvae to light. *Zoolog Sci* 20(1):13–22.
22. Nakayama-Ishimura A, Chambon JP, Horie T, Satoh N, Sasakura Y (2009) Delineating metamorphic pathways in the ascidian Ciona intestinalis. *Dev Biol* 326(2):357–367.
23. Hollmann M, Heinemann S (1994) Cloned glutamate receptors. *Annu Rev Neurosci* 17:31–108.
24. Schwenk J, et al. (2014) Regional diversity and developmental dynamics of the AMPA-receptor proteome in the mammalian brain. *Neuron* 84(1):41–54.
25. Belachew S, Gallo V (2004) Synaptic and extrasynaptic neurotransmitter receptors in glial precursors' quest for identity. *Glia* 48(3):185–196.
26. Nicol D, Meinertzhagen IA (1991) Cell counts and maps in the larval central nervous system of the ascidian *Ciona intestinalis* (L.). *J Comp Neurol* 309(4):415–429.
27. Krupnick JG, Benovic JL (1998) The role of receptor kinases and arrestins in G protein-coupled receptor regulation. *Annu Rev Pharmacol Toxicol* 38:289–319.
28. Kusakabe T, et al. (2001) Ci-opsin1, a vertebrate-type opsin gene, expressed in the larval ocellus of the ascidian Ciona intestinalis. *FEBS Lett* 506(1):69–72.
29. Kusakabe T, Tsuda M (2007) Photoreceptive systems in ascidians. *Photochem Photobiol* 83(2):248–252.
30. Walker CS, et al. (2006) Conserved SOL-1 proteins regulate ionotropic glutamate receptor desensitization. *Proc Natl Acad Sci USA* 103(28):10787–10792.

31. Wang R, et al. (2008) Evolutionary conserved role for TARPs in the gating of glutamate receptors and tuning of synaptic function. *Neuron* 59(6):997–1008.
32. Walker CS, et al. (2006) Reconstitution of invertebrate glutamate receptor function depends on stargazin-like proteins. *Proc Natl Acad Sci USA* 103(28):10781–10786.
33. Nicoll RA, Tomita S, Bredt DS (2006) Auxiliary subunits assist AMPA-type glutamate receptors. *Science* 311(5765):1253–1256.
34. Ziff EB (2007) TARPs and the AMPA receptor trafficking paradox. *Neuron* 53(5): 627–633.
35. Jonas P, Burnashev N (1995) Molecular mechanisms controlling calcium entry through AMPA-type glutamate receptor channels. *Neuron* 15(5):987–990.
36. Verdoorn TA, Burnashev N, Monyer H, Seeburg PH, Sakmann B (1991) Structural determinants of ion flow through recombinant glutamate receptor channels. *Science* 252(5013):1715–1718.
37. Hume RI, Dingledine R, Heinemann SF (1991) Identification of a site in glutamate receptor subunits that controls calcium permeability. *Science* 253(5023):1028–1031.
38. Sommer B, Köhler M, Sprengel R, Seeburg PH (1991) RNA editing in brain controls a determinant of ion flow in glutamate-gated channels. *Cell* 67(1):11–19.
39. Swanson GT, Kamboj SK, Cull-Candy SG (1997) Single-channel properties of recombinant AMPA receptors depend on RNA editing, splice variation, and subunit composition. *J Neurosci* 17(1):58–69.
40. Nutt SL, Kamboj RK (1994) Differential RNA editing efficiency of AMPA receptor subunit GluR-2 in human brain. *Neuroreport* 5(13):1679–1683.
41. Whitney NP, et al. (2008) Calcium-permeable AMPA receptors containing Q/R-unedited GluR2 direct human neural progenitor cell differentiation to neurons. *FASEB J* 22(8):2888–2900.
42. Wahlstedt H, Daniel C, Ensterö M, Ohman M (2009) Large-scale mRNA sequencing determines global regulation of RNA editing during brain development. *Genome Res* 19(6):978–986.
43. Venø MT, et al. (2012) Spatio-temporal regulation of ADAR editing during development in porcine neural tissues. *RNA Biol* 9(8):1054–1065.
44. Pachernegg S, Münster Y, Muth-Köhne E, Fuhrmann G, Hollmann M (2015) GluA2 is rapidly edited at the Q/R site during neural differentiation *in vitro*. *Front Cell Neurosci* 9:69.
45. Kawahara Y, et al. (2004) Glutamate receptors: RNA editing and death of motor neurons. *Nature* 427(6977):801.
46. Kwak S, Hideyama T, Yamashita T, Aizawa H (2010) AMPA receptor-mediated neuronal death in sporadic ALS. *Neuropathology* 30(2):182–188.
47. Peng PL, et al. (2006) ADAR2-dependent RNA editing of AMPA receptor subunit GluR2 determines vulnerability of neurons in forebrain ischemia. *Neuron* 49(5): 719–733.
48. Schmidt HD, et al. (2015) ADAR2-dependent GluA2 editing regulates cocaine seeking. *Mol Psychiatry* 20(11):1460–1466.
49. Brusa R, et al. (1995) Early-onset epilepsy and postnatal lethality associated with an editing-deficient GluR-B allele in mice. *Science* 270(5242):1677–1680.
50. Chen YC, et al. (2001) Identifications, classification, and evolution of the vertebrate alpha-amino-3-hydroxy-5-methyl-4-isoxazole propionic acid (AMPA) receptor subunit genes. *J Mol Evol* 53(6):690–702.
51. Shepherd JD, Huganir RL (2007) The cell biology of synaptic plasticity: AMPA receptor trafficking. *Annu Rev Cell Dev Biol* 23:613–643.
52. Nishida H (1987) Cell lineage analysis in ascidian embryos by intracellular injection of a tracer enzyme. III. Up to the tissue restricted stage. *Dev Biol* 121(2):526–541.
53. Eagleson GW, Harris WA (1990) Mapping of the presumptive brain regions in the neural plate of Xenopus laevis. *J Neurobiol* 21(3):427–440.
54. Kajiwara S, Yoshida M (1985) Changes in behavior and ocellar structure during the larval life of solitary ascidians. *Biol Bull* 169:565–577.
55. Bone Q (1992) On the locomotion of ascidian tadpole larvae. *J Mar Biol Assoc U K* 72: 161–186.
56. Foster RG, Roberts A (1982) The pineal eye in Xenopus laevis embryos and larvae: A photoreceptor with a direct excitatory effect on behavior. *J Comp Physiol* 145: 413–419.
57. Mick G (1995) Non-N-methyl-D-aspartate glutamate receptors in glial cells and neurons of the pineal gland in a higher primate. *Neuroendocrinology* 61(3):256–264.
58. Kaur C, Sivakumar V, Ling EA (2005) Expression of N-methyl-D-aspartate (NMDA) and alpha-amino-3-hydroxy-5-methyl-4-isoxazolepropionate (AMPA) GluR2/3 receptors in the developing rat pineal gland. *J Pineal Res* 39(3):294–301.
59. Horie T, Orii H, Nakagawa M (2005) Structure of ocellus photoreceptors in the ascidian *Ciona* intestinalis larva as revealed by an anti-arrestin antibody. *J Neurobiol* 65(3):241–250.
60. Jansson LC, Wigren HK, Nordström T, Akerman KE (2011) Functional α-amino-3-hydroxy-5-methylisoxazole-4-propionic acid receptors in differentiating embryonic neural progenitor cells. *Neuroreport* 22(6):282–287.
61. Maric D, et al. (2000) Functional ionotropic glutamate receptors emerge during terminal cell division and early neuronal differentiation of rat neuroepithelial cells. *J Neurosci Res* 61(6):652–662.
62. Hsu WL, et al. (2015) Glutamate stimulates local protein synthesis in the axons of rat cortical neurons by activating α-amino-3-hydroxy-5-methyl-4-isoxazolepropionic acid (AMPA) receptors and metabotropic glutamate receptors. *J Biol Chem* 290(34): 20748–20760.
63. Fannon J, Tarmier W, Fulton D (2015) Neuronal activity and AMPA-type glutamate receptor activation regulates the morphological development of oligodendrocyte precursor cells. *Glia* 63(6):1021–1035.
64. Catsicas M, Allcorn S, Mobbs P (2001) Early activation of Ca(2+)-permeable AMPA receptors reduces neurite outgrowth in embryonic chick retinal neurons. *J Neurobiol* 49(3):200–211.
65. Poluch S, et al. (2001) AMPA receptor activation leads to neurite retraction in tangentially migrating neurons in the intermediate zone of the embryonic rat neocortex. *J Neurosci Res* 63(1):35–44.
66. Sutherland ML, Delaney TA, Noebels JL (1996) Glutamate transporter mRNA expression in proliferative zones of the developing and adult murine CNS. *J Neurosci* 16(7): 2191–2207.
67. Furuta A, Rothstein JD, Martin LJ (1997) Glutamate transporter protein subtypes are expressed differentially during rat CNS development. *J Neurosci* 17(21):8363–8375.
68. Hartfuss E, Galli R, Heins N, Götz M (2001) Characterization of CNS precursor subtypes and radial glia. *Dev Biol* 229(1):15–30.
69. Tosti E, Boni R, Gallo A (2016) Ion currents in embryo development. *Birth Defects Res C Embryo Today* 108(1):6–18.
70. Rosenberg SS, Spitzer NC (2011) Calcium signaling in neuronal development. *Cold Spring Harb Perspect Biol* 3(10):a004259.
71. Nakajo K, Nishino A, Okamura Y, Kubo Y (2011) KCNQ1 subdomains involved in KCNE modulation revealed by an invertebrate KCNQ1 orthologue. *J Gen Physiol* 138(5): 521–535.
72. Miledi R, Parker I (1984) Chloride current induced by injection of calcium into Xenopus oocytes. *J Physiol* 357:173–183.
73. Miledi R (1982) A calcium-dependent transient outward current in Xenopus laevis oocytes. *Proc R Soc Lond B Biol Sci* 215(1201):491–497.
74. Barish ME (1983) A transient calcium-dependent chloride current in the immature Xenopus oocyte. *J Physiol* 342:309–325.
75. Yamada L, et al. (2003) Morpholino-based gene knockdown screen of novel genes with developmental function in Ciona intestinalis. *Development* 130(26):6485–6495.
76. Hotta K, et al. (2007) A web-based interactive developmental table for the ascidian Ciona intestinalis, including 3D real-image embryo reconstructions: I. From fertilized egg to hatching larva. *Dev Dyn* 236(7):1790–1805.
77. Corbo JC, Levine M, Zeller RW (1997) Characterization of a notochord-specific enhancer from the Brachyury promoter region of the ascidian, Ciona intestinalis. *Development* 124(3):589–602.
78. Horie T, Nakagawa M, Orii H, Tsuda M (2002) Whole structure of the photoreceptors in the ascidian larva visualized by an antibody against arrestin (Ci-Arr). *J Photosci* 19: 272–274.
79. Tsuda M, Sakurai D, Goda M (2003) Direct evidence for the role of pigment cells in the brain of ascidian larvae by laser ablation. *J Exp Biol* 206(Pt 8):1409–1417.